CHEMISTRY
A EUROPEAN JOURNAL

DOI: 10.1002/chem.201000198

Self-Assembly and Structural Evolvement of Polyoxometalate-Anchored Dendron Complexes

Yang Yang, Yizhan Wang, Haolong Li, Wen Li, and Lixin Wu*[a]

Abstract: A cationic dendritic molecule that has alkyl chains has been synthesized and employed to encapsulate anionic polyoxometalates through electrostatic interactions. The prepared surfactant-encapsulated polyoxometalate (SEP) complexes were used as building blocks to fabricate self-assemblies in solution and the solid state. Monodispersion, lamellar, and columnar assemblies of SEP complexes have been characterized in detail. With increasing the number of peripheral cationic dendrons on inorganic clusters, the SEPs undergo changes from globular assemblies to monodispersions in solution and from lamellar assemblies to hexagonal columnar structures in the solid state, depending on the amounts of cationic dendrons in the complexes. The structural evolvement was simulated through consideration of the size and shape of the cationic dendron and polyanionic clusters, and the experimental results are in good agreement with the interpretation of the simulations. The present research demonstrates a new kind of dendritic complex and provides a route for controlling their assembling states by simply alternating the number of cationic dendrons in the complexes.

Keywords: dendrimers · hybrid dendritic complexes · polyoxometalates · self-assembly · structural evolvement

Introduction

Dendritic molecules represent a family of well-defined, three-dimensional branched architectures and are widely used for the construction of nanostructures and various self-assemblies because their size, shape, flexibility, and surface chemistry can be precisely controlled at the molecular level.[1] Diverse self-assemblies composed of dendritic molecules such as micelles, vesicles, tubes, and columnar structures have been developed through suitable molecular designs. The unique properties of dendritic molecules, especially those combining functional units, exhibit potential applications in nanomaterials,[2] biomimic,[3] drug delivery,[4] and catalysis.[5] To simplify synthetic procedures and particularly to obtain functional dendritic systems, many components including photochromic and luminescent groups, amino acids, metal ions, and metal and/or semiconductor nanoparticles have been grafted into dendritic architectures through non-covalent bonds, such as hydrogen bond, host-guest recognition, coordination, and electrostatic interactions.[2a] Thus, the ability to combine multicomponents in one dendritic unit that can create new features in addition to the sum of the individual parts is of special interest.

Polyoxometalates (POMs) are discrete, molecularly defined inorganic metal–oxide clusters with structural variety and interesting functional properties leading to rich applications in catalysis, optics, magnetics, and medicine.[6] Moreover, as intriguing inorganic building blocks with uniform nanoscale size (one to several nanometers), versatile negative charges, and topologic morphologies, POMs have been employed for the fabrication of organic–inorganic hybrid materials.[7] Among the strategies for the modification of POMs, a facile and simple approach currently used to fabricate POM-based organic–inorganic hybrid complexes is to replace the counterions of POMs by cationic surfactants, resulting in surfactant-encapsulated POMs (SEPs).[8] An SEP complex possessing a discrete supramolecular architecture that has a hydrophobic shell and a hydrophilic POM core in a well-defined composition can lead to increased stability of inner POMs,[9] improved photophysical properties,[10] enhanced biological activity,[11] and can especially make POMs soluble in weak and nonpolar organic solvents, which is very useful for the fabrication of POM-based film devices.[8a] Linear single- and double-chain cationic surfactants[12] have

[a] Y. Yang, Y. Wang, Dr. H. Li, Dr. W. Li, Prof. L. Wu
State Key Laboratory of Supramolecular Structure and Materials
College of Chemistry, Jilin University, Changchun 130012 (China)
Fax: (+86) 431-8519-3421
E-mail: wulx@jlu.edu.cn

Supporting information for this article is available on the WWW under http://dx.doi.org/10.1002/chem.201000198.

been employed to enwrap POMs, and the formed SEPs were successfully applied in the self-assemblies. Most of SEPs tend to assemble into lamellar structures in solution, except in a very few cases of hexagonal or cubic structures through using a special POM and a specially designed surfactant.[8a,13] It has been attempted to incorporate POMs into dendritic architectures and the resulting complexes were supposed to exhibit homogeneous catalysis for the epoxidation of dienes.[14]

In contrast to the reported results, the assembly of POMs connected to dendritic molecules in organic solution has been little mentioned. From a self-assembly point of view, POMs can also be employed to adjust the self-assembly behavior of dendritic molecules through the formation of precisely defined complexes. This strategy reveals several merits: The variable size and abundant shapes of POMs match the requirement of the precise structure of dendritic complexes and the changeable surface charges of POMs can be used to change the amount of dendrons in one complex architecture. In addition, binding with dendritic molecules is favorable for the self-assembly of POMs in soft organic matrices in a designed way, which is normally uncontrollable in simply mixing systems. As a result, the dendritic shell can have an impact on the access of small molecules to the inorganic core, which may result in the special effects of enzymelike regioselectivity and substrate selectivity.[15] However, to the best of our knowledge, the matching relationship between cationic dendrons and POMs has never been involved and applied to tune the existing states in solution and the self-assembled structures in the solid state. Herein we report the self-assembly behavior of a new class of SEP complexes, $D_4SiW_{12}O_{40}$ (SEP-D_4), $D_5BW_{12}O_{40}$ (SEP-D_5), $D_7MSiW_{11}O_{39}$ (M = Na or K; SEP-D_7), and $D_{10}Na_2P_2W_{15}O_{56}$ (SEP-D_{10}), containing different numbers of cationic dendritic molecules (D) around POM cores as shown in Scheme 1. It was found that the existing states of the dendritic complexes in solution transformed from an aggregated state to a monodisperse state with increasing the number of combined cationic dendrons. Meanwhile, the complexes changed their shapes from rodlike to disklike in the solid state, and as a result the self-assembled structures varied from lamellar to hexagonal columnar arrays. The proposed assembled structures were manipulated and displayed unusual agreement with the experimental data.

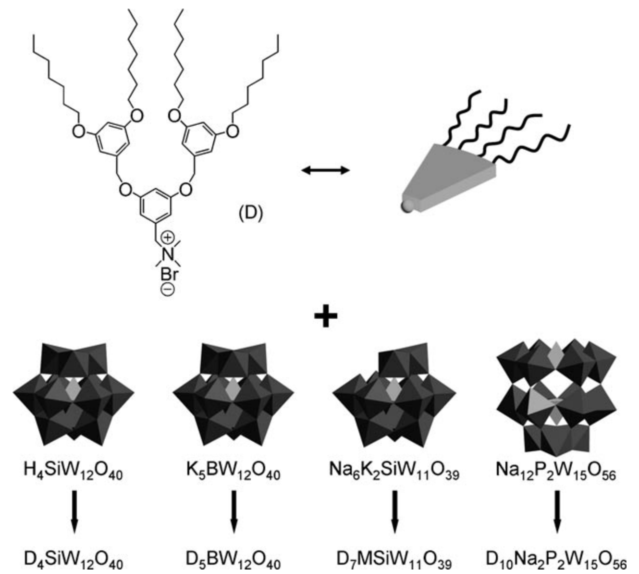

Scheme 1. The chemical structure of dendritic molecule (D) and schematic polyhedrons of four POMs.

Results and Discussion

Preparation and characterization of SEPs: The dendritic molecule that has four heptyl chains, denoted as D, was synthesized and characterized (see Figures S1–S3 in the Supporting Information) as described in detail in the Experimental Section. To evaluate the influence of the number of cationic dendrons in the complexes on the self-assembly behavior in solution and the formed assembled structures in the solid state, we chose four types of anionic POMs with nearly the same size and morphology but with different numbers of charges to be encapsulated. Both POM-1 and POM-2 are Keggin-type heteropolytungstates, whereas POM-3 is a monolacunary Keggin-type heteropolytungstate, and POM-4 is a trilacunary Dawson-type heteropolytungstate, the size of which is a little bigger than the Keggin-type POMs. The preparation of the POMs and SEPs was carried out by following the procedures described in the literature.[16,17] The main purpose of introducing alkyl chains into the dendritic molecule is to increase the flexibility and assembling ability of the complexes. The four corresponding POMs are soluble in water, and in contrast all of the as-prepared SEPs are immiscible in water but readily dissolve in organic media such as cyclohexane, toluene, chloroform, and acetone, suggesting that the POMs have been successfully encapsulated by dendritic molecules.

The elemental analysis results suggest the chemical formulae of SEP-D_4, SEP-D_5, SEP-D_7, and SEP-D_{10} to be $D_4SiW_{12}O_{40}$ (6151.05), $D_5BW_{12}O_{40}$ (6953.00), $D_7Na(SiW_{11}O_{39})$ (8431.88) or $D_7K(SiW_{11}O_{39})$ (8447.99), and $D_{10}Na_2P_2W_{15}O_{56}$ (11953.76). The thermogravimetric (TG) results of SEP-D_4, SEP-D_5, SEP-D_7, and SEP-D_{10} show 53.3, 60.8, 69.4, and 69.8% mass loss before 900°C, which matches well with the expected values, 53.8, 60.0, 68.7–68.5, and 70.4%, respectively, which are calculated from each corresponding chemical formula by assuming that the organic component has decomposed completely and that the POMs have transformed into the corresponding oxides. Combining the elemental analysis and TG results, we infer that the chemical formulae of SEPs are consistent with the expected target products. As for SEP-D_7, we could not recognize the residue metal ion as being a sodium or potassium cation owing to the very low content in the complex and very little difference between the two expected formulae. Actually, the uncertainty does not affect the composition and self-assembling property of the complex, therefore, further confirmation was not carried out.

^{1}H NMR spectra of SEP-D_4, SEP-D_5, SEP-D_7, and SEP-D_{10} confirm the presence of cationic dendrons on the encapsulated clusters. In contrast to NMR signals of the dendritic molecule alone, those of cationic dendrons in SEP-D_4 show the following changes: 1) Except for the proton peak of Ar*H* that is *ortho* to $-CH_2OAr$ at the 2,6-positions, the other proton peaks have significantly broadened and shifted to high field, especially those near the nitrogen atom. For example, the proton peak of the *N*-methyl group has remarkably broadened and shifted toward high field by 0.16 ppm, and the proton peak of the *N*-methylene group has evidently broadened and shifted to high field by 0.50 ppm. 2) The proton peak of the Ar*H* group that is *para* to $-CH_2N(CH_3)_3$ at the 4-position, which should split into a triplet, becomes a considerably broadened singlet and is shifted to a higher field by 0.09 ppm. 3) The proton peak of the Ar*H* group that is *ortho* to $-CH_2N(CH_3)_3$ at the 2,6-positions, which should split into a doublet, becomes a highly broadened singlet and shifts to higher field by 0.14 ppm. We also observed similar broadening and shifting of the NMR signals of the cationic dendrons in other SEPs. The peak broadening and shifting clearly result from the strong electrostatic interactions between the cationic dendrons and the POMs, which restricts the mobility of the cationic dendrons on the surface of the POMs in the organic phase, especially for their ammonium head parts.[13a,18]

As shown in the IR spectra (Figure S6 in the Supporting Information), the bands appearing at 2927–2929 and 2856 cm^{-1} are assigned to CH_2 antisymmetric and symmetric stretching modes of alkyl chains, respectively. Meanwhile, the bands at 1597–1599, 1483–1484, and 1456 cm^{-1} can be clearly assigned to the benzyl framework, C−N scissoring, and CH_2 scissoring modes, respectively. In addition, the bands of the W-O_c-W vibrations shift from 787–814 and 735–739 cm^{-1} in the free POMs to 800–829 and 729–758 cm^{-1} in the SEPs, the vibrations of W-O_b-W change from 879–937 cm^{-1} in the free POMs to around 885–937 cm^{-1} in the SEPs, and the W−O_d stretches transfer from 978–1001 and 945–958 cm^{-1} in the free POMs to 972–993 and 940–951 cm^{-1} in the SEPs. These vibration bands (assigned and summarized in Table S1 in the Supporting Information) indicate that, on the one hand, the frame structures of POMs are well kept, and on the other hand, the strong electrostatic interaction occurs between the cationic dendrons and the POMs.[19]

Self-assemblies of dendritic molecules and SEPs in solution: From the previous results and related reports concerning the assembly of surfactant-enwrapped complexes, it is known that the solvent polarity plays an important role for the stabilization of self-assembled structures and the creation of novel assembling morphologies.[12b] We tried several weak polar solvents and found consistent assembling morphology for the as-prepared complexes. The addition of polar solvents can increase the stability of the assemblies in solution so that the self-assemblies keep their structures well even after the evaporation of solvent. Thus, the addition of methanol or ethanol becomes necessary to solidify the self-assembled structures of SEPs in chloroform. As a substitution and a monocomponent solvent, acetone serves the same role for the structural characterization of the assemblies in solution systems. To evaluate the effect of the organic component covering on POMs for the assemblies of SEPs, we initially investigated the self-assembling behavior of the dendritic molecule in organic solution. TEM measurements (Figure 1 a) demonstrate that the dendritic ammonium cation is not singularly molecularly dispersed but that it is in an aggregated state in acetone, and vesicular aggregations are clearly observed with a size scale in the range of 20–30 nm. The wall thickness of the vesicular assemblies is approximately 3.0 nm, which is accordance with the length of two ideal dendritic molecules ($L_D = 1.6$ nm) estimated from the data in the literature.[20] The XRD pattern further demonstrates that the dendritic molecule forms a lamellar structure. As seen in Figure 1 b, two Bragg diffraction peaks appear at 2.86 and 5.78°, corresponding to the layer spacings of 3.1 and 1.5 nm, respectively, which can be well indexed as (001) and (002) reflections of a lamellar structure with a layer spacing of 3.1 nm. Combining the length of two dendritic molecules, the total thickness of a single bilayer is estimated to be approximately 3.2 nm. It is known that the frequencies of CH_2 antisymmetric and symmetric stretching bands are sensitive to the conformation of alkyl chains: Low wavenumbers (2915–2918 and 2846–2850 cm^{-1}) are characteristic of a highly *trans* conformation of alkyl chains,[21] whereas their upward shifts (2924–2929 and 2854–2856 cm^{-1}) are indicative of the increase in *gauche* conformers, implying that the alkyl chain conformation tends to disorder. On the basis of this, the observed frequencies of 2929 and 2856 cm^{-1} of the dendritic molecules indicate the pres-

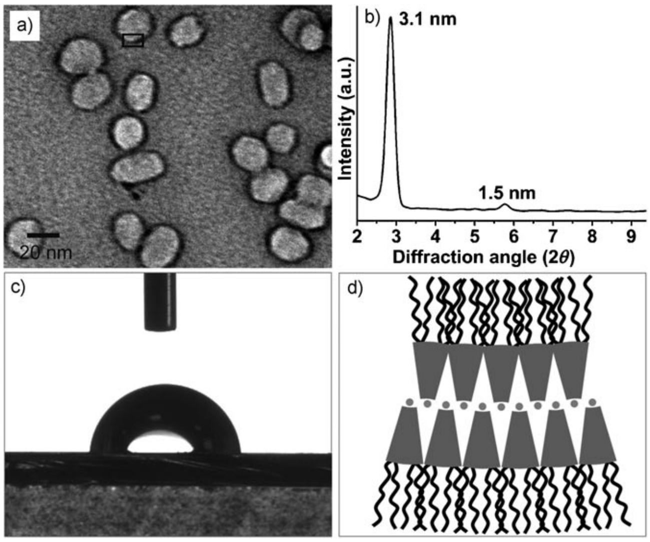

Figure 1. a) TEM image of dendritic molecule assemblies prepared from acetone solution (1 $mg\,mL^{-1}$), b) XRD pattern of casting dendron assemblies, c) the shape of a water droplet on the surface of casting dendron assemblies on a silica substrate, and d) schematic representation for the reverse-bilayer structure of vesicular assemblies.

ence of *gauche* conformers and the disorder of the alkyl chain conformation. Considering the disordered conformation of the alkyl chains and the lateral hydrophobic compressing for the dendritic molecules standing in the layer, it is reasonable that the measured layer distance (3.1 nm) is approximate to the ideal layer spacing (3.2 nm). The static contact angle (Figure 1 c) of the dendritic molecule assemblies for water is approximately 86°, showing a hydrophobic surface. These results imply that the vesicular assemblies possess a reverse-bilayer structure with the alkyl chains facing the acetone solvent and, therefore, a schematic assembling model of the dendritic molecule has been proposed in Figure 1 d.

From the dynamic light scattering (DLS) results in Figure 2, it can be seen that SEP-D_4 and SEP-D_5 are in an aggregated state in acetone, with the hydrodynamic diameters of approximately 396 and 122 nm, respectively. Contrary

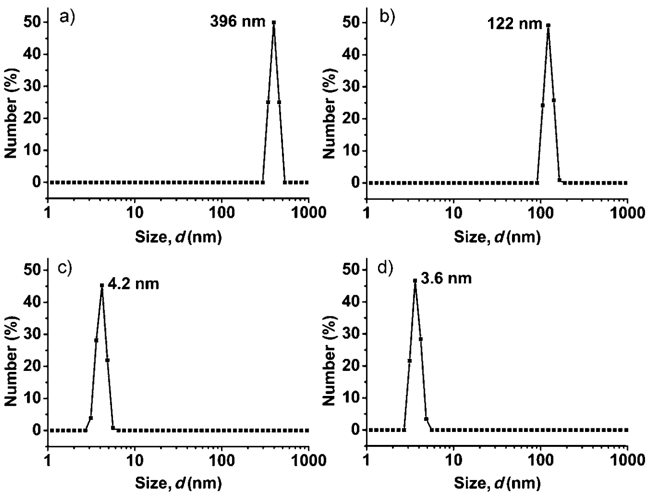

Figure 2. DLS diagrams of a) SEP-D_4, b) SEP-D_5, c) SEP-D_7, and d) SEP-D_{10} in acetone solution with a concentration of 1 $mg\,mL^{-1}$.

to what is expected, by increasing the number of cationic dendrons around the POMs we observed that SEP-D_7 and SEP-D_{10} are clearly amorphous in acetone, rather than in an aggregated state, because the observed hydrodynamic diameters are 4.2 and 3.6 nm, respectively, which are very small and approximate to the size scale of a single complex. TEM and SEM images of SEP-D_4 (Figure 3 a and Figure S7 a in the Supporting Information) reveal that the complex assemblies have a spherical shape, and the diameter determined from these measurements is consistent with the DLS results. The precise structure of these spheres of SEP-D_4 cannot be observed by TEM successfully because the assemblies are quite solid and the electron beam cannot penetrate the objects. The TEM and SEM results (Figure 3 b and S7b in the Supporting Information) of SEP-D_5 demonstrate consistent phenomena with that of SEP-D_4. However, SEP-D_7 and SEP-D_{10} complexes do not form clear aggregations in acetone, as demonstrated by their TEM images shown in Figure 3 c and d, respectively, which is in accordance with the DLS results. Interestingly, SEP-D_7 appears as a separated

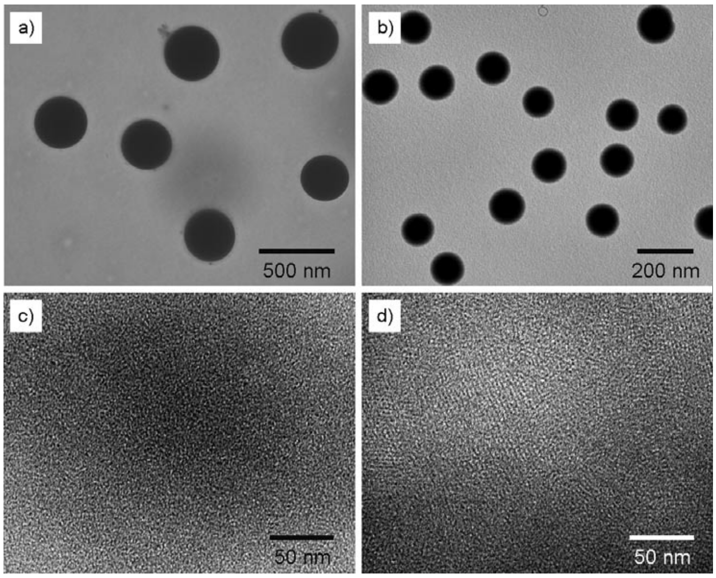

Figure 3. TEM images of a) SEP-D_4, b) SEP-D_5, c) SEP-D_7, and d) SEP-D_{10} in acetone solution with a concentration of 1 $mg\,mL^{-1}$.

dark spot with the diameter scale of approximately 3–4 nm, which is in agreement with the exact size of the complex. The results for SEP-D_{10} are similar to those of SEP-D_7. The difference of assembling properties for these two SEPs from SEP-D_4 and SEP-D_5 could be reasonably explained as deriving from the change of the cationic dendron number on the periphery of the POMs. The complexes containing less cationic dendrons have enough space to reorganize themselves and assemble together and this is driven by hydrophobic forces, whereas the complexes that have more cationic dendrons are able to remain apart from each other in solution, resulting in the monodispersed state.

To understand the self-assembled structure of the spherical assemblies of SEP-D_4 and SEP-D_5 further, XRD was employed for further characterization and the results (Figure 4) show that the lamellar structures exist in both spherical assemblies of SEP-D_4 and SEP-D_5. Three diffraction peaks in the XRD pattern of SEP-D_4 (Figure 4 a) appear at 2.76 (001), 5.48 (002), and 8.18° (003), suggesting a layered structure with thickness 3.2 nm. The intensity of the (003) reflection is a bit stronger than the (002) reflec-

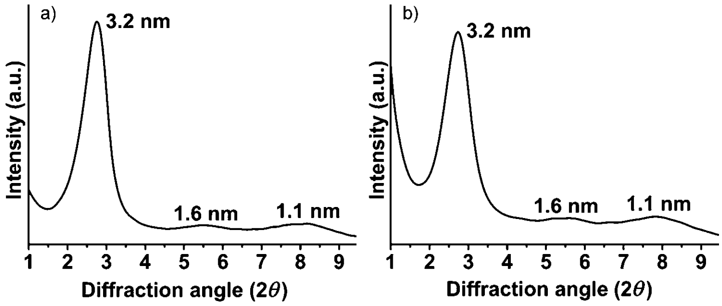

Figure 4. XRD patterns of the assemblies of a) SEP-D_4 and b) SEP-D_5 complexes prepared from acetone solution.

tion, indicating a symmetrical double-layered structure.[12g] Combining the diameter of one Keggin-type POM (1.0 nm) and the length of two cationic dendrons (3.2 nm), the ideal diameter of one SEP-D_4 complex is about 4.2 nm, which is much larger than the measured layer distance. Because the CH_2 symmetric and antisymmetric stretching vibrations for SEP-D_4 appear at 2856 and 2929 cm^{-1}, respectively, the shorter layer spacing should be mainly derived from the conformation disorder of alkyl chains.[21] Note that the layer spacing of the dendritic complex is close to that of the precursor dendron. Based on the present experimental data, it is difficult to explain the phenomenon reliably. However, it is possible that the rigid POM clusters support the bending of the cationic dendrons with enough space to make the packing looser than dendritic molecules alone, leading to a shorter bilayer length (2.2 nm) than the measured layer distance (3.1 nm) of separated dendritic molecules. Likewise, SEP-D_5 displays a similar lamellar structure and consistent layer spacing with the estimated results. The static contact angles (Figure S8 in the Supporting Information) of dry SEP-D_4 and SEP-D_5 castings for water are 102 and 99°, respectively, indicating a hydrophobic surface composed of alkyl chains. Thus, spherical assemblies of these two complexes are deduced as possessing a vesiclelike structure with reverse bilayers, as previously fabricated by different complexes.[12b] Again, in agreement with the TEM observation, we did not find any diffractions belonging to lamellar structures in the XRD data of SEP-D_7 and SEP-D_{10}, further confirming that more cationic dendrons covering the POMs can lead to a change of the assembled structure of SEPs.

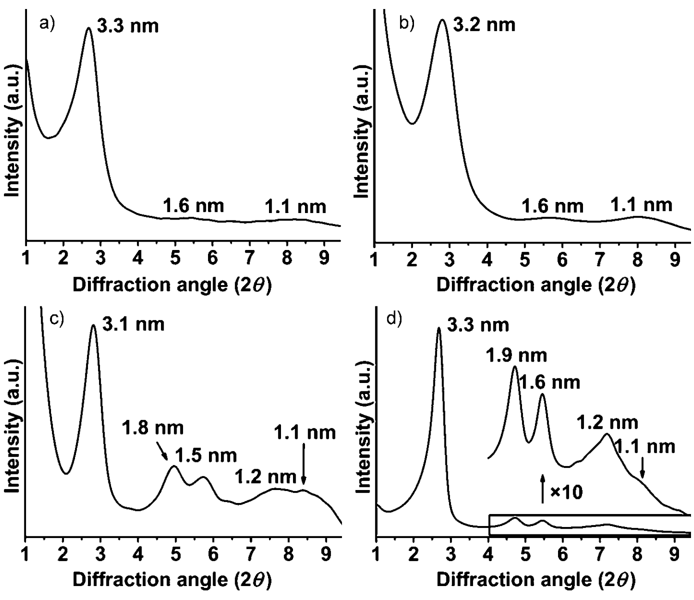

Figure 5. XRD patterns of a) SEP-D_4, b) SEP-D_5, c) SEP-D_7, and d) SEP-D_{10} assemblies in the solid state.

Self-assemblies of SEPs in the solid state: To investigate the solvent effect on the self-assembled structures during the evaporation, we examined the solid structures of SEP complexes prepared through directly drying the sample solutions. The XRD results in Figure 5 a and b demonstrate that the solids of SEP-D_4 and SEP-D_5 prepared from chloroform possess similar lamellar structures to those from acetone solution, whereas we could not observe the globular assembling morphologies seen in Figure 3. Considering the instability of SEP-D_4 and SEP-D_5 assemblies during solvent evaporation, which is due to the weak interaction between complexes, it is possible that the vesicular assemblies that occurred in chloroform collapse into lamellar structures in the solid state, as for the case found in a previous report.[12b] Three Bragg diffractions in the XRD pattern of SEP-D_4 (Figure 5 a) appear at 2.68 (001), 5.44 (002), and 8.20° (003), supporting the assignment of a lamellar structure. However, the layer spacing of 3.3 nm is much smaller than the ideal layer distance but it is in accordance with the layer spacing of the assemblies in acetone implying the unchanged transfer of the assemblies. Again, having a slightly stronger (003) reflection than a (002) reflection indicates that the solid assemblies possess a symmetrical double-layered structure.[12g] Similarly, the IR spectrum of SEP-D_4 reveals the disordered conformation of the alkyl chains in SEP-D_4 solid because of the symmetric and antisymmetric stretching vibrations of the CH_2 group emerging at 2856 and 2929 cm^{-1},[21] which should be the main reason for the shorter layer distance. From these results and from the fact that strong phase segregation occurs between the hydrophilic POM-1 cores and the hydrophobic dendrons, we can propose a self-assembled structure of SEP-D_4 in the solid state (Scheme 2 b), that is, the cationic dendrons are piled on two opposite sides of inorganic clusters and extend along the layer direction under the packing interaction. This rodlike reorganization of the complex in shape is, of course, favorable for tight parallel organization. The POM-1 clusters constituting the central layer embedded by cationic dendrons further assemble into a lamellar structure. SEP-D_5 also has a lamellar structure, and its XRD pattern (Figure 5 b) exhibits a layer spacing of

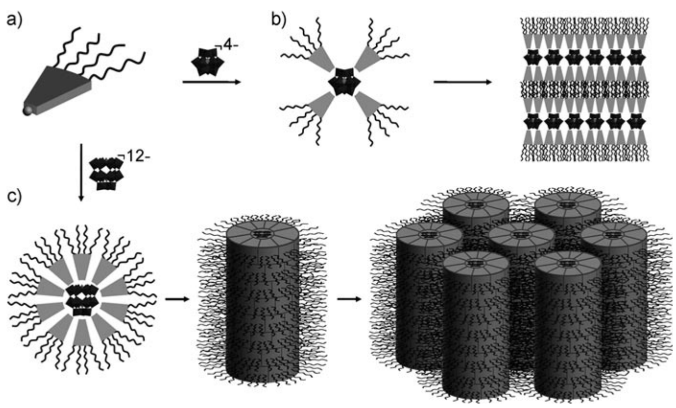

Scheme 2. Schematic representation of a) dendritic molecule D, b) the complex SEP-D_4 and its bilayer structure, in which these complex units are accommodated in the layers without packing curvature, and c) the complex SEP-D_{10} and its hexagonal columnar structure, in which the complex adapts itself to an oblate shape to form the hexagonally packed cylinders instead of layers.

3.2 nm, almost the same as that of SEP-D_4. Interestingly, through carefully dispersing a solid powder of SEP-D_4 and SEP-D_5, the assembled structures can be further identified from TEM images (Figure 6a and b) in which a clearly layered structure is found with an estimated layer spacing of approximately 3.0 nm, which is in perfect agreement with the value estimated from the XRD data.

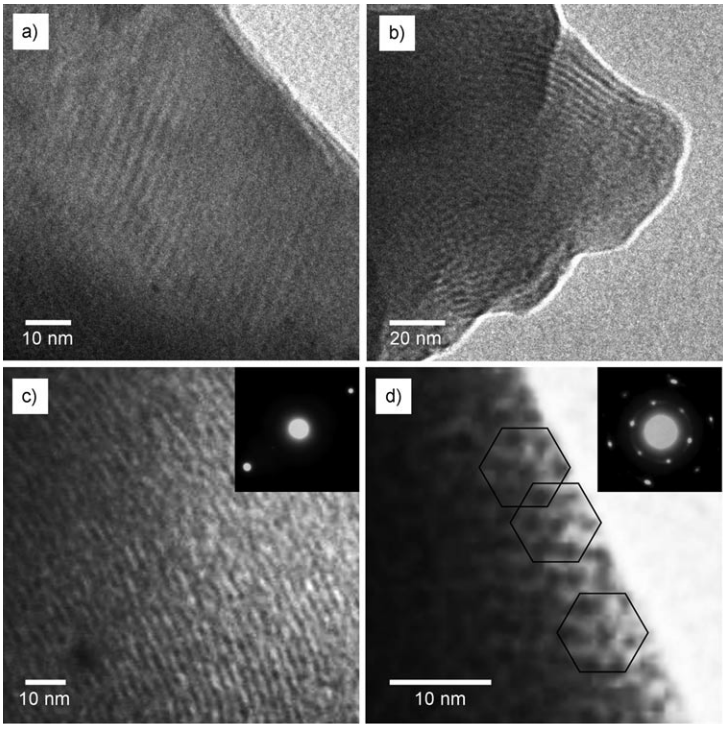

Figure 6. TEM images of a) SEP-D_4, b) SEP-D_5, c) SEP-D_7 viewed perpendicular to the columnar direction, and d) SEP-D_7 viewed parallel to the columnar direction. The insets in c) and d) are the corresponding electron diffraction patterns.

Very interestingly, in contrast to the nonstructured state in solution, we observed the self-assembled structures of SEP-D_7 and SEP-D_{10} in their solid states. Compared with the lamellar assemblies of SEP-D_4 and SEP-D_5, the XRD pattern of SEP-D_7 in Figure 5c exhibits five diffraction peaks at 2.82 (100), 4.96 (110), 5.72 (200), 7.64° (210), and 8.38° (300), which can be well indexed to a hexagonal columnar structure with a lattice parameter of $a = 3.6$ nm ($2d_{100}/\sqrt{3}$). Consistent with the case in which the layer length is much smaller than the ideal diameter of SEP-D_4 and SEP-D_5, the length of the a axis is also much smaller than the estimated ideal value (4.2 nm) of one monolacunary Keggin-type POM (1.0 nm) and two cationic dendrons (3.2 nm). The XRD pattern (Figure 5d) of SEP-D_{10} suggests a similar hexagonal columnar structure with a lattice parameter of $a = 3.8$ nm. Considering that CH_2 symmetric and antisymmetric stretching vibrations appear at 2856 and 2927 cm^{-1}, respectively, the conformation of alkyl chains of cationic D dendrons in SEP-D_7 and SEP-D_{10} is quite disordered, apparently leading to the smaller intercolumnar distance. Summarizing these factors, we propose a packing model for SEP-D_7 and SEP-D_{10} in the solid state as presented in Scheme 2c. The hexagonal columnar structure matches the face-to-face stacking of the two SEPs in a disklike shape, and the flexible alkyl chains on the periphery fill the space between the columns. The hydrophilic regions of the complexes interact preferably with each other and, therefore, segregate from the hydrophobic regions into distinct domains. The segregation effects between hydrophilic and hydrophobic components should be one of the main driving forces for the formation of a columnar structure. The hexagonal packing modes of SEP-D_7 and SEP-D_{10} are supported by the TEM characterization. From the high-resolution TEM images of SEP-D_7, we clearly observed both the linear structure (Figure 6c) and the lateral hexagonal spots (Figure 6d). The dark POM domain is clearly surrounded by the light organic region, and the intercolumnar distance is approximately 3.4 nm from the magnified TEM image, which is in good agreement with the lattice parameter of the a axis derived from the XRD results. The electron diffractions of the planform and side view (insets of Figure 6c and d) of the assemblies are in a linear and a hexagonal fashion, respectively, further confirming the assignment. Thus, we can see that SEP-D_7 and SEP-D_{10} complexes prefer to form hexagonal columnar assemblies rather than lamellar assemblies in the solid state when they are prepared from chloroform. So far, there are very few reports about the columnar phases based on SEPs,[13a–c] and to the best of our knowledge this is an unprecedented example of the hexagonal columnar self-assembled structures formed by SEPs with small-sized POMs.

Discussion of self-assembled structures and structural evolvement: The above results indicate that with increasing the number of cationic dendrons around the POMs, a structural evolvement takes place from lamellar to hexagonal columns in the solid state. Because the employed POMs are similar in size and morphology, the molecular geometry of the cationic dendron and its number covering on the POMs, as well as its array on the periphery of the SEPs, become the crucial factors in determining the self-assembled structures and morphologies of the SEPs in solution and the solid state. Here, we try to discuss the possible mechanism for understanding such a structural evolvement.

Similar to liquid-crystal systems,[22] the orientation and array of the cationic dendrons in SEPs have important effects on the self-assembled structures. In view of the feasible rearrangement on the exterior of POMs, the dendrons can adopt different orientation states depending on the free space around the POM cores owing to the requirement for tight assembly. Under the conditions of similar size and morphology of the POMs, increasing the number or the density of cationic dendrons leads to a larger surface occupation (or a smaller free space) and definite changes of the shape and packing state of SEPs accordingly. In this case, the accommodation of SEP complexes confined within the rod shape for lamellar array becomes unlikely. Therefore, the SEPs that have seven or ten cationic dendrons adopt an oblate orientation instead of the parallel distribution that is found in the lamellar assemblies of SEP-D_4 and SEP-D_5. With such an orientation, the SEPs have to transform into a disklike state and then stack into columns, which further self-assemble parallel to each other in a regular manner to form a hexagonal two-dimensional array. The orientation state of the cationic dendrons can be approximately predicted by volume calculations by filling the periphery of the SEPs.

For a convenient comprehension, we divided the POM cluster into six regions similar to the faces of a cube, as shown in Scheme 3a. The maximum possessive volume (V) of cationic dendrons can be divided into six units, corresponding to the cube faces during the solvent-driven phase separation. For the lamellar structures, the cationic dendrons were forced into two opposite facets, whereas for the hexagonal columnar structures, the dendrons were instead pressed to occupy four adjacent facets in a rather flat disklike shape, which enabled the most efficient interaction of the hydrophilic regions of neighboring complexes. For the SEP forming the lamellar structure, the maximum possessive volume (V_l) of the dendrons should be two of the six units, that is, $V/3$, whereas for the SEP forming the hexagonal columnar structure, the maximum occupied volume (V_h) of the dendrons would be four of the six units, that is, $2V/3$. As a result, the hexagonal columnar structure can form only when the total volume of cationic dendrons (V_{Dn}) is in agreement with $V_l < V_{Dn} \leq V_h$. From Scheme 3b, V can be calculated according to Equation (1), in which r_1 denotes the radius of POM, and r_2 is the radius of SEP.

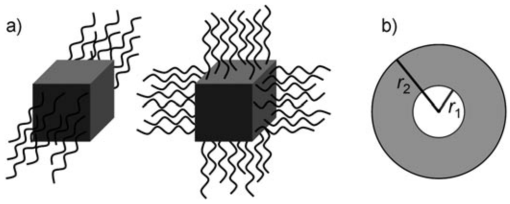

Scheme 3. a) Supposed cubic models with two opposite facets occupied for the lamellar structure and four adjacent facets filled for the 2D hexagonal columnar structure, and b) the organic shell of the SEP (the dark ring represents the organic shell composed of cationic dendrons, r_1 represents the radius of the POM, and r_2 represents the radius of the SEP).

$$V = 4\pi(r_2^3 - r_1^3)/3 \quad (1)$$

According to the similar size of the POMs in the present study, r_1 is approximately 0.5 nm and r_2 is equal to $a/2$, which can be estimated from the lattice parameter of the hexagonal columnar structure of SEP-D_7. Thus, Equation (1) provides the calculated V of 23.9 nm^3. Accordingly, V_l is 8.0 nm^3 and V_h is 16.0 nm^3. The volume of the cationic dendron (V_D) can be estimated to be 1.3 nm^3 by employing a similar dendritic molecule as that in reference [20]. Therefore, the volumes of the organic parts of SEP-D_4, SEP-D_5, SEP-D_7, and SEP-D_{10} should be $V_{D4} = 5.2$, $V_{D5} = 6.5$, $V_{D7} = 9.1$, and $V_{D10} = 13.0$ nm^3, respectively. From these calculated volumes, it is easy to find that both V_{D4} and V_{D5} are smaller than V_l, whereas the values of V_{D7} and V_{D10} are located just between V_l and V_h. The former two complexes should self-assemble into lamellar structures, and owing to the space limit for the latter two complexes, the layered structures no longer remain and break into tight hexagonal columnar packing structures. The larger occupation of the cationic dendrons in SEP-D_7 and SEP-D_{10} with respect to that in SEP-D_4 and SEP-D_5 makes these two complexes favor organization into columnar assemblies, leading to the tight hexagonal packing structures. The main driving forces can be suitably ascribed to the phase segregation of incompatible units (the hydrophilic POM core and hydrophobic dendritic part), the aggregation of compatible units, and the minimization of volume.[23] In contrast to the present results, through increasing the number of the linear surfactants such as dioctadecyldimethylammonium bromide (DODA),[12b–d] the yielding lamellar structure does not change at all. This is because the DODA skeletons are greatly flexible and incomplete for steric constraints. So, the dendritic surfactants play a special and irreplaceable role in the structural evolvement owing to their rigidity and divergent shape. It is clear that the balance between the formation of the lamellar structures and hexagonal columnar structures can be finely tuned by manipulating the number of cationic dendrons on the periphery of the SEPs.

Conclusion

As a whole, the dendritic molecule that has four heptyl chains was synthesized, and four types of dendritic surfactant-encapsulated polyoxometalates containing different numbers of cationic dendrons were prepared depending on the charges of the POMs. We found that SEP-D_4 and SEP-D_5 complexes, which have a low number of cationic dendrons, self-assemble into vesicular aggregations with lamellar structures in acetone, whereas with a relatively high number of cationic dendrons, SEP-D_7 and SEP-D_{10} complexes become monodisperse in acetone solution and exhibit hexagonal columnar structures in the solid state. The branched molecular structure of the cationic dendron and the matching relationship between the cationic dendrons and POMs plays an important role in the formation of hexagonal columnar structures. A mechanism of the structural evolvement based on the orientation change of the cationic dendrons on the periphery of SEPs as a result of their varied number in one complex has been proposed, and the type of self-assembled structures can be effectively predicted through comparing the total volume of the dendrons in one complex with their maximum possessive volumes for the lamellar and hexagonal columnar structures. Therefore, we identify a facile and feasible route to control the assembled structures in solution and in the solid state by modifying the number of the cationic dendrons on the periphery of SEPs. Furthermore, the above-mentioned structural evolvement concept may provide a general pathway to construct other types of self-assemblies based on POMs such as the cubic-packed structure by further increasing the number of the peripheral cationic dendrons in one SEP. These self-assembled structures are promising structures for use as supramolecular soft templates that may contribute to unique effects on the catalytic, optical, and magnetic properties of POMs.

Experimental Section

Materials: $H_4SiW_{12}O_{40}$ (POM-1) was purchased from Sinopharm Chemical Reagent and was used as received. The other POMs, $K_5BW_{12}O_{40}$ (POM-2), $K_6Na_2SiW_{11}O_{39}$ (POM-3), and $Na_{12}P_2W_{15}O_{56}$ (POM-4) were freshly prepared according to the literature procedures.[16] 3,5-Dihydroxybenzoic acid was obtained from Alfa Aesar and 3,5-dihydroxybenzyl alcohol was obtained from ACROS. All of the starting compounds for synthesis were used without further purification, and all of the used solvents were analytical grade. Doubly distilled water was used in the experiments. Silica gel (100–200 mesh) was used for column chromatography.

Synthesis of dendritic molecule D: The cationic dendritic quaternary ammonium bearing four heptyl chains was synthesized step by step by using the convergent method.[24] The detailed synthetic procedures are described in Scheme 4. The chemical structure of the dendritic molecule was confirmed by FTIR and ^{1}H NMR spectroscopy, as well as MALDI-TOF mass spectrometry.

Methyl 3,5-dihydroxybenzoate (1): 3,5-Dihydroxybenzoic acid (10.0 g, 65.0 mmol), methanol (150 mL), and *p*-toluene sulfonic acid (3.0 g, 17.4 mmol) were mixed and stirred under reflux for 20 h in a N_2 atmosphere. The excess methanol was removed through rotary evaporation, and then the reaction mixture was redissolved in hot water. The insoluble impurities were filtered out, and the filtrate was cooled to room temperature to give a white crystalline solid (yield: 6.1 g, 56.0%). ^{1}H NMR ($CDCl_3$, TMS): $\delta = 3.89$ (s, 3H; -COOCH_3), 4.86 (s, 2H; O*H*-Ar), 6.56 (t, $J = 2$ Hz, 1H; Ar*H* *para* to -$COOCH_3$ at the 4-position), 7.09 ppm (d, $J = 2$ Hz, 2H; Ar*H* *ortho* to -$COOCH_3$ at the 2,6-positions).

Methyl 3,5-bis(heptyloxy)benzoate (2): n-Heptyl bromide (42.6 g, 237.9 mmol), **1** (10.0 g, 59.5 mmol), anhydrous K_2CO_3 (24.7 g, 178.7 mmol), 18-crown-6 (32.3 mg), and acetone (150 mL) were mixed together, and the mixture was stirred under reflux in a N_2 atmosphere for 24 h. Then, the reaction mixture was monitored by TLC analysis and cooled to room temperature. The solid salts were filtered out, and the solvent in the filtrate was evaporated under reduced pressure. The liquid mixture was then purified by using silica-gel column chromatography (eluent: 1:1 (v/v) chloroform/cyclohexane) to give a colorless liquid (yield: 14.8 g, 68.8%). ^{1}H NMR ($CDCl_3$, TMS): $\delta = 0.89$ (t, $J = 6.5$ Hz, 6H; -CH_3), 1.29–38 (m, 12H; -(CH_2)$_3$-), 1.41–1.47 (m, 4H; -CH_2-CH_3), 1.74–1.78 (m, 4H; -CH_2-CH_2-O-Ar), 3.89 (s, 3H; -COOCH_3), 3.96 (t, $J = 6.5$ Hz, 4H; -CH_2-O-Ar), 6.63 (t, $J = 2$ Hz, 1H; Ar*H* *para* to -$COOCH_3$ at the 4-position), 7.15 ppm (d, $J = 2$ Hz, 2H; Ar*H* *ortho* to -$COOCH_3$ at the 2,6-positions).

3,5-Bis(heptyloxy)benzyl alcohol (3): A solution of **2** (2.0 g, 5.5 mmol) in distilled THF (10 mL) was added dropwise to a stirred suspension of $LiAlH_4$ (0.3 g, 7.9 mmol) in distilled THF (40 mL) in an ice-water bath. After the addition, the mixture was stirred for an additional 24 h at room temperature. The reaction was then quenched by the successive addition of 95% ethanol (ca. 50 mL) and water (ca. 2 mL). The insoluble impuri-

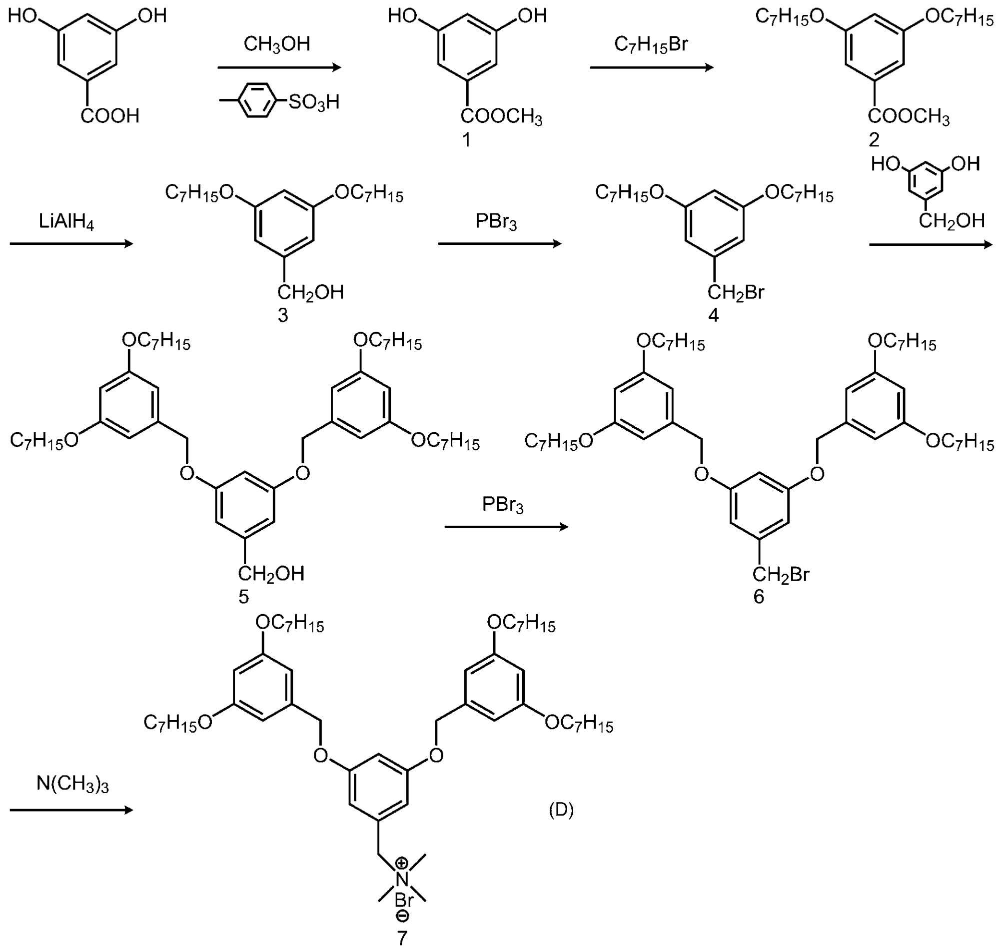

Scheme 4. Synthetic route of the dendritic molecule D.

ties were filtered out. The residual solution was extracted with chloroform (3×50 mL), and the combined chloroform solution was then dried and evaporated under reduced pressure to dryness to give a yellow liquid. The crude product was purified by using silica-gel column chromatography (eluent: chloroform) to give a light-yellow liquid (yield: 1.7 g, 92.1 %). ^{1}H NMR (CDCl$_3$, TMS): δ=0.89 (t, J=6.5 Hz, 6H; -CH_3), 1.30–1.34 (m, 12H; -(CH_2)$_3$-), 1.42–1.45 (m, 4H; -CH_2-CH$_3$), 1.75–1.77 (m, 4H; -CH_2-CH$_2$-O-Ar), 3.93 (t, J=6 Hz, 4H; -CH_2-O-Ar), 4.62 (s, 2H; -CH_2-OH), 6.37 (s, 1H; ArH *para* to -CH$_2$OH at the 4-position), 6.50 ppm (s, 2H; ArH *ortho* to -CH$_2$OH at the 2,6-positions).

3,5-Bis(heptyloxy)benzyl bromide (4): Compound **3** (1.5 g, 4.4 mmol) was dissolved in dry benzene (50 mL) and was cooled to 0–5 °C in an ice-water bath. PBr$_3$ (0.2 mL, 2.1 mmol) was added dropwise with stirring. The mixture was stirred for another 6 h at room temperature, and doubly distilled water (30 mL) was added to quench the reaction. The benzene in the reaction solution was evaporated under vacuum, and the mixture was extracted with dichloromethane (3×30 mL). The combined extracts were dried with anhydrous sodium sulfate and evaporated to dryness. The crude product was purified by using silica-gel column chromatography (eluent: 1:1 (v/v) dichloroform/cyclohexane) to give a light-yellow thick liquid product (yield: 1.7 g, 95.5 %). ^{1}H NMR (CDCl$_3$, TMS): δ= 0.89 (t, 6H; -CH_3), 1.30–1.34 (m, 12H; -(CH_2)$_3$-), 1.42–1.45 (m, 4H; -CH_2-CH$_3$), 1.75–1.77 (m, 4H; -CH_2-CH$_2$-O-Ar), 3.92 (t, 4H; -CH_2-O-Ar), 4.41 (s, 2H; -CH_2-Br), 6.37 (s, 1H; ArH *para* to -CH$_2$Br at the 4-position), 6.51 ppm (s, 2H; ArH *ortho* to CH$_2$Br at the 2,6-positions).

3',5'-Bis(3,5-bis(heptyloxy)benzyloxy)benzyl alcohol (5): Compound **4** (1.7 g, 4.3 mmol), 3,5-dihydroxybenzyl alcohol (0.25 g, 1.8 mmol), anhydrous K$_2$CO$_3$ (1.0 g, 7.2 mmol), and catalytic amount of 18-crown-6 were dissolved in acetone (50 mL) and the mixture was stirred under reflux in a N$_2$ atmosphere for 24 h. The reaction was monitored by TLC analysis. The reaction mixture was filtered and the excess solvent was evaporated. The liquid mixture was then purified by using silica-gel column chromatography (eluent: 10:1 (v/v) cyclohexane/ethyl acetate) to give a light-yellow thick liquid (yield: 1.0 g, 72.1 %). ^{1}H NMR ([D$_6$]DMSO, TMS): δ=0.86 (t, J=6.5 Hz, 12H; -CH_3), 1.24–1.41 (m, 32H; -(CH_2)$_4$-CH$_3$), 1.65–1.70 (m, 8H; -CH_2-CH$_2$-O-Ar), 3.92 (t, 8H; J=6.5 Hz, -CH_2-O-Ar), 4.41 (d, J=6 Hz, 2H; -CH_2-OH), 4.97 (s, 4H; Ar-CH_2-O-Ar), 5.18 (t, J= 6 Hz, 1H; -OH), 6.39 (t, J=2 Hz, 2H; ArH *para* to -CH$_2$OAr at the 4-position), 6.49 (t, 1H; ArH *para* to -CH$_2$OH at the 4-position), 6.54–6.55 ppm (m, 4H and 2H; ArH *ortho* to -CH$_2$OAr at the 2,6-positions and ArH *ortho* to -CH$_2$OH at the 2,6-positions).

3',5'-Bis(3,5-bis(heptyloxy)benzyloxy)benzyl bromide (6): This compound was prepared from compound **5** by using a reaction procedure similar to the preparation of compound **4**. The crude product was directly used in the following step without purification.

***N*-3',5'-bis(3,5-bis(heptyloxy)benzyloxy)benzyl-*N*,*N*,*N*-trimethylammonium bromide (D)**: An aqueous solution of trimethylamine (33 %, 0.7 g, 3.9 mmol) and crude product **6** (0.5 g) were dissolved in ethanol (50 mL), and the mixture was stirred under reflux for 24 h with monitoring by TLC analysis. The excess solvent and most of trimethylamine were evaporated under vacuum. The thick liquid mixture was then purified by using silica-gel column chromatography (eluent: 20:1 (v/v) chloroform/methanol) to give a ceraceous solid (yield: 0.4 g, 69.1 % over two steps). ^{1}H NMR (CDCl$_3$, TMS): δ=0.89 (t, J=6.5 Hz, 12H; -CH_3), 1.28–1.46 (m, 32H; -(CH_2)$_4$-CH$_3$), 1.73–1.79 (m, 8H; -CH_2-CH$_2$-O-Ar), 3.32 (s, 9H; (CH_3)$_3$N), 3.94 (t, J=6.5 Hz, 8H; -CH_2-O-Ar), 4.89 (s, 2H; -CH_2-N-(CH$_3$)$_3$), 4.99 (s, 4H; Ar-CH_2-O-Ar), 6.39 (t, J=2 Hz, 2H; ArH *para* to -CH$_2$OAr at the 4-position), 6.55 (d, J=2 Hz, 4H; ArH *ortho* to -CH$_2$OAr at the 2,6-positions), 6.71 (t, 1H; ArH *para* to -CH$_2$N(CH$_3$)$_3$ at the 4-position), 6.83 ppm (d, J=2 Hz, 2H; ArH *ortho* to -CH$_2$N(CH$_3$)$_3$ at the 2,6-positions); MALDI-TOF MS: m/z: 819.4 [M^+]; IR (KBr): $\tilde{\nu}$= 3423, 2954, 2929, 2856, 1597, 1488, 1462, 1379, 1167, 1059 cm^{-1}.

Preparation of SEPs: All SEP complexes were prepared at room temperature according to the previously reported procedures,[17] and were confirmed by ^{1}H NMR and IR spectroscopy, elemental analysis, and TG measurements.

SEP-D$_4$: A solution of dendritic molecule D (0.1 g) in chloroform (50 mL) was added dropwise into an aqueous solution (50 mL) of POM-1 (0.09 g) under stirring, and its initial molar ratio to POM-1 was controlled at 3.8:1. The organic phase was separated, washed with water (3×30 mL) and dried over anhydrous sodium sulfate. SEP-D$_4$ was obtained by evaporating the chloroform to dryness. The product was stored in a vacuum desiccator until the weight remained constant (yield: 0.14 g, 82.4 %). ^{1}H NMR (CDCl$_3$, TMS): δ=0.85 (t, J=6.5 Hz, 12H; -CH_3), 1.25–1.40 (m, 32H; -(CH_2)$_4$-CH$_3$), 1.68–1.73 (m, 8H; -CH_2-CH$_2$-O-Ar), 3.16 (s, 9H; (CH_3)$_3$N), 3.89 (t, J=6 Hz, 8H; -CH_2-O-Ar), 4.39 (s, 2H; -CH_2-N(CH$_3$)$_3$), 4.92 (s, 4H; Ar-CH_2-O-Ar), 6.34 (s, 2H; ArH *para* to -CH$_2$OAr at the 4-position), 6.56 (s, 4H; ArH *ortho* to -CH$_2$OAr at the 2,6-positions), 6.62 (s, 1H; ArH *para* to -CH$_2$N(CH$_3$)$_3$ at the 4-position), 6.69 ppm (s, 2H; ArH *ortho* to -CH$_2$N(CH$_3$)$_3$ at the 2,6-positions); IR (KBr): $\tilde{\nu}$=3435, 2954, 2929, 2856, 1597, 1484, 1456, 1377, 1167, 1059, 972, 924, 885, 800 cm^{-1}; elemental analysis (%) calcd for SEP-D$_4$ (C$_{208}$H$_{336}$N$_4$O$_{64}$W$_{12}$Si, 6151.05): C 40.61, H 5.51, N 0.91; found: C 41.30, H 5.59, N 0.92 (corresponding to the chemical formula: D$_4$SiW$_{12}$O$_{40}$ (6151.05)); the TG measurement displays a 53.3 % (w/w) mass loss between 40 and 600 °C.

SEP-D$_5$: The complex was prepared by following a similar procedure as for SEP-D$_4$, but by using POM-2 instead of POM-1. The initial molar ratio of dendritic molecule D to POM-2 was kept at 4.5:1 (yield: 0.03 g, 76.9 %). ^{1}H NMR (CDCl$_3$, TMS): δ=0.86 (t, J=6.5 Hz, 12H; -CH_3), 1.26–1.39 (m, 32H; -(CH_2)$_4$-CH$_3$), 1.70 (s, 8H; -CH_2-CH$_2$-O-Ar), 3.17 (s, 9H; (CH_3)$_3$N), 3.89 (s, 8H; -CH_2-O-Ar), 4.45 (s, 2H; -CH_2-N(CH$_3$)$_3$), 4.93 (s, 4H; Ar-CH_2-O-Ar), 6.35 (s, 2H; ArH *para* to -CH$_2$OAr at the 4-position), 6.56 (s, 4H; ArH *ortho* to -CH$_2$OAr at the 2,6-positions), 6.61 (s, 1H; ArH *para* to -CH$_2$N(CH$_3$)$_3$ at the 4-position), 6.77 ppm (s, 2H; ArH *ortho* to -CH$_2$N(CH$_3$)$_3$ at the 2,6-positions); IR (KBr): $\tilde{\nu}$=3440, 2954, 2929, 2856, 1599, 1483, 1456, 1379, 1165, 1059, 993, 951, 903, 829 cm^{-1}; elemental analysis (%) calcd for SEP-D$_5$ (C$_{260}$H$_{420}$N$_5$O$_{70}$W$_{12}$B, 6953.00): C 44.91, H 6.09, N 1.01; found: C 45.72, H 5.85, N 0.64 (corresponding to the chemical formula: D$_5$BW$_{12}$O$_{40}$ (6953.00)); the TG measurement displays a 60.8 % (w/w) mass loss between 45 and 600 °C.

SEP-D$_7$: The complex was prepared by following a similar procedure as for SEP-D$_4$, but by using POM-3 instead of POM-1. The initial molar ratio of dendritic molecule D to POM-3 was controlled at 6.5:1 (yield: 0.10 g, 78.1 %). ^{1}H NMR (CDCl$_3$, TMS): δ=0.85 (t, J=6.5 Hz, 12H; -CH_3), 1.25–1.36 (m, 32H; -(CH_2)$_4$-CH$_3$), 1.68 (s, 8H; -CH_2-CH$_2$-O-Ar), 3.14 (s, 9H; (CH_3)$_3$N), 3.84 (s, 8H; -CH_2-O-Ar), 4.49 (s, 2H; -CH_2-N-(CH$_3$)$_3$), 4.87 (s, 4H; Ar-CH_2-O-Ar), 6.32 (s, 2H; ArH *para* to -CH$_2$OAr at the 4-position), 6.51 (s, 4H and 1H; ArH *ortho* to -CH$_2$OAr at the 2,6-positions and ArH *para* to -CH$_2$N(CH$_3$)$_3$ at the 4-position), 6.76 ppm (s, 2H; ArH *ortho* to -CH$_2$N(CH$_3$)$_3$ at the 2,6-positions); IR (KBr): $\tilde{\nu}$=3433, 2954, 2927, 2856, 1599, 1484, 1456, 1379, 1165, 1059, 993, 940, 889, 802, 729 cm^{-1}; elemental analysis (%) calcd for SEP-D$_7$ (C$_{364}$H$_{588}$N$_7$O$_{81}$W$_{11}$SiNa or C$_{364}$H$_{588}$N$_7$O$_{81}$W$_{11}$SiK, 8431.88 or 8447.99): C 51.85 or 51.75, H 7.03 or 7.02, N 1.16 or 1.16; found: C 51.52, H 7.00, N 0.58 (corresponding to the chemical formula: D$_7$Na(SiW$_{11}$O$_{39}$) (8431.88) or D$_7$K(SiW$_{11}$O$_{39}$) (8447.99)); the TG measurement displays a 69.4 % (w/w) mass loss between 45 and 600 °C.

SEP-D$_{10}$: The complex was prepared by following a similar procedure as for SEP-D$_4$, but by using POM-4 instead of POM-1. The initial molar ratio of dendritic molecule D to POM-4 was controlled at 8:1 (yield: 0.08 g, 88.9 %). ^{1}H NMR (CDCl$_3$, TMS): δ=0.86 (t, J=6.5 Hz, 12H; -CH_3), 1.26–1.38 (m, 32H; -(CH_2)$_4$-CH$_3$), 1.70 (s, 8H; -CH_2-CH$_2$-O-Ar), 3.22 (s, 9H; (CH_3)$_3$N), 3.87 (s, 8H; -CH_2-O-Ar), 4.49 (s, 2H; -CH_2-N-(CH$_3$)$_3$), 4.88 (s, 4H; Ar-CH_2-O-Ar), 6.34 (s, 2H; ArH *para* to -CH$_2$OAr at the 4-position), 6.53 (s, 4H; ArH *ortho* to -CH$_2$OAr at the 2,6-positions), 6.58 (s, 1H; ArH *para* to -CH$_2$N(CH$_3$)$_3$ at the 4-position), 6.70 ppm (s, 2H; ArH *ortho* to -CH$_2$N(CH$_3$)$_3$ at the 2,6-positions); IR (KBr): $\tilde{\nu}$=3435, 2954, 2927, 2856, 1599, 1484, 1456, 1379, 1167, 1122, 1080, 1059, 972, 937, 889, 816, 758 cm^{-1}; elemental analysis (%) calcd for SEP-D$_{10}$ (C$_{520}$H$_{840}$N$_{10}$O$_{116}$W$_{15}$P$_2$Na$_2$, 11953.76): C 52.25, H 7.08, N 1.17; found: C 52.00, H 6.37, N 1.00 (corresponding to the chemical formula: D$_{10}$Na$_2$P$_2$W$_{15}$O$_{56}$ (11953.76)); the TG measurement displays a 69.8 % (w/w) mass loss between 45 and 900 °C.

Sample preparation for measurements: For the identification of the self-assembled structures of dendritic molecule D and SEPs from acetone solution, all of the sample films for XRD measurement were prepared through direct casting of the dendritic molecule D or SEP solutions (0.5 mL, 1 $mg\,mL^{-1}$) onto silica substrates at ambient temperature. For measurements of the self-assembled structures in the solid states, owing to the poor solubility in ethanol all of the as-prepared SEPs were suspended in ethanol by undergoing ultrasonic treatment. Taking SEP-D_7 as an example, the sample (1.0 mg) was added to ethanol (2.0 mL) and the mixture was sonicated for 30 min. The sample film for XRD measurement was prepared by directly casting 1 mL of the above mixture dispersion onto a silica substrate at ambient temperature. For identifying the existing states of SEPs in acetone solution, all of the specimens for TEM measurement were prepared through dropping some of the SEP solutions (1 $mg\,mL^{-1}$) onto the carbon-coated copper grids, which were then dried through suction of the excess sample solutions with filter paper at room temperature. For the self-assembled structures in the solid state, the SEP samples for TEM measurement were prepared in the same way as the samples for XRD measurement. Taking SEP-D_7 as an example, SEP-D_7 (1.0 mg) was added to ethanol (2.0 mL) and the mixture was sonicated for 30 min. Several drops of the dispersion were placed onto the carbon-coated copper grid and dried through suction of the excess sample solution with filter paper.

Measurements: ^{1}H NMR spectra were recorded on a Bruker Avance 500 instrument by using TMS as an internal reference. IR spectral measurements on pressed KBr pellets were performed on a Bruker IFS66v FT-IR spectrometer equipped with a DGTS detector (32 scans) with a resolution of 4 cm^{-1}. Element analysis (C, H, N) was carried out on a Flash EA1112 analyzer from ThermoQuest Italia S.P.A. TG thermograms were conducted on a Perkin–Elmer Diamond TG/DTA instrument with a heating rate of 10 °C min^{-1} under flowing air. MALDI-TOF mass spectra were recorded on a LDI-1700 mass spectrometer (Linear Scientific) with chloroform as the solvent. XRD patterns were collected on a Rigaku X-ray diffractometer (D/max rA, using $Cu_{K\alpha}$ radiation at 1.542 Å), and the data were recorded from 0.5 to 10°. TEM images were obtained with a Hitachi H8100 electron microscope with accelerating voltage of 200 kV without staining. SEM measurements were performed on a JEOL JSM-6700F field-emission scanning electron microscope. DLS measurements were performed by using a Zetasizer NanoZS (Malvern Instruments). The contact angles were carried out on a Drop Shape Analysis System DSA20MK2 KRÜSS (Edward Keller) at 25 °C. The amount of one droplet of water that was used for the measurement was approximately 3 μL.

Acknowledgements

This work was financially supported by the National Basic Research Program of China (2007CB808003), the National Natural Science Foundation of China (20973082, 20921003, 20703019), and MOST. We thank the 111 Project (B06009) for supporting the visit of Prof. I. Kim at Pusan National University who provided fruitful discussion, as well as the Open Project of State Key Laboratory of Polymer Physics and Chemistry of the CAS.

[1] D. Schröder, M. Diefenbach, T. M. Klapötke, H. Schwarz, *Angew. Chem.* **1990**, *102*, 119–157; *Angew. Chem. Int. Ed. Engl.* **1990**, *29*, 138–175.

[2] a) D. K. Smith, A. R. Hirst, C. S. Love, J. G. Hardy, S. V. Brignell, B. Huang, *Prog. Polym. Sci.* **2005**, *30*, 220–293; b) B. Donnio, S. Buathong, I. Bury, D. Guillon, *Chem. Soc. Rev.* **2007**, *36*, 1495–1513; c) Special issue "Dendrimers and Nanoscience": D. Astruc, *C. R. Chim.* **2003**, *6*, 709–711.

[3] J. Kofoed, J. L. Reymond, *Curr. Opin. Chem. Biol.* **2005**, *9*, 656–664.

[4] U. Boas, P. M. H. Heegaard, *Chem. Soc. Rev.* **2004**, *33*, 43–63.

[5] D. Astruc, F. Chardac, *Chem. Rev.* **2001**, *101*, 2991–3023.

[6] a) M. T. Pope, A. Müller, *Angew. Chem.* **1991**, *103*, 56–70; *Angew. Chem. Int. Ed. Engl.* **1991**, *30*, 34–48; b) Special issue on "Polyoxometalates": *Chem. Rev.* **1998**, *98*, 1–390.

[7] a) W. Qi, Y. Wang, W. Li, L. Wu, *Chem. Eur. J.* **2010**, *16*, 1068–1078; b) H. Li, W. Qi, W. Li, H. Sun, W. Bu, L. Wu, *Adv. Mater.* **2005**, *17*, 2688–2692; c) W. Qi, H. Li, L. Wu, *Adv. Mater.* **2007**, *19*, 1983–1987; d) Y. Han, Y. Xiao, Z. Zhang, B. Liu, P. Zheng, S. He, W. Wang, *Macromolecules* **2009**, *42*, 6543–6548; e) W. Bu, H. Li, H. Sun, S. Yin, L. Wu, *J. Am. Chem. Soc.* **2005**, *127*, 8016–8017; f) H. Zhang, X. Lin, Y. Yan, L. Wu, *Chem. Commun.* **2006**, 4575–4577.

[8] a) D. G. Kurth, P. Lehmann, D. Volkmer, H. Cölfen, M. J. Koop, A. Müller, A. Du Chesne, *Chem. Eur. J.* **2000**, *6*, 385–393; b) W. Bu, H. Fan, L. Wu, X. Hou, C. Hu, G. Zhang, X. Zhang, *Langmuir* **2002**, *18*, 6398–6403.

[9] S. Nlate, D. Astruc, R. Neumann, *Adv. Synth. Catal.* **2004**, *346*, 1445–1448.

[10] W. Bu, L. Wu, X. Zhang, A.-C. Tang, *J. Phys. Chem. B* **2003**, *107*, 13425–13431.

[11] R. Carr, I. A. Weinstock, A. Sivaprasadarao, A. Müller, A. Aksimentiev, *Nano Lett.* **2008**, *8*, 3916–3921.

[12] a) M. Nyman, M. A. Rodriguez, T. M. Anderson, D. Ingersoll, *Cryst. Growth Des.* **2009**, *9*, 3590–3597; b) H. Li, H. Sun, W. Qi, M. Xu, L. Wu, *Angew. Chem.* **2007**, *119*, 1322–1325; *Angew. Chem. Int. Ed.* **2007**, *46*, 1300–1303; c) H. Sun, H. Li, W. Bu, M. Xu, L. Wu, *J. Phys. Chem. B* **2006**, *110*, 24847–24854; d) Y. Wang, W. Li, L. Wu, *Langmuir* **2009**, *25*, 13194–13200; e) Y. Yan, B. Li, W. Li, H. Li, L. Wu, *Soft Matter* **2009**, *5*, 4047–4053; f) W. Li, W. Bu, H. Li, L. Wu, M. Li, *Chem. Commun.* **2005**, 3785–3787; g) W. Li, S. Yin, J. Wang, L. Wu, *Chem. Mater.* **2008**, *20*, 514–522; h) S. Yin, W. Li, J. Wang, L. Wu, *J. Phys. Chem. B* **2008**, *112*, 3983–3988; i) T. Akutagawa, R. Jin, R. Tunashima, S. Noro, L. Cronin, T. Nakamura, *Langmuir* **2008**, *24*, 231–238.

[13] a) S. Polarz, B. Smarsly, M. Antonietti, *ChemPhysChem* **2001**, *2*, 457–461; b) T. Zhang, C. Spitz, M. Antonietti, C. F. J. Faul, *Chem. Eur. J.* **2005**, *11*, 1001–1009; c) X. Lin, Y. Wang, L. Wu, *Langmuir* **2009**, *25*, 6081–6087; d) D. Volkmer, A. Du Chesne, D. G. Kurth, H. Schnablegger, P. Lehmann, M. J. Koop, A. Müller, *J. Am. Chem. Soc.* **2000**, *122*, 1995–1998.

[14] D. Volkmer, B. Bredenkötter, J. Tellenbröker, P. Kögerler, D. G. Kurth, P. Lehmann, H. Schnablegger, D. Schwahn, M. Piepenbrink, B. Krebs, *J. Am. Chem. Soc.* **2002**, *124*, 10489–10496.

[15] a) R. Brodbeck, T. Tönsing, D. Andrae, D. Volkmer, *J. Phys. Chem. B* **2008**, *112*, 5153–5162; b) S. Nlate, L. Plault, D. Astruc, *Chem. Eur. J.* **2006**, *12*, 903–914.

[16] a) I. A. Weinstock, J. J. Cowan, E. M. G. Barbuzzi, H. Zeng, C. L. Hill, *J. Am. Chem. Soc.* **1999**, *121*, 4608–4617; b) N. Haraguchi, Y. Okaue, T. Isobe, Y. Matsuda, *Inorg. Chem.* **1994**, *33*, 1015–1020; c) B. J. Hornstein, R. G. Finke, *Inorg. Chem.* **2002**, *41*, 2720–2730.

[17] a) C. F. J. Faul, M. Antonietti, *Adv. Mater.* **2003**, *15*, 673–683; b) H. Li, P. Li, Y. Yang, W. Qi, H. Sun, L. Wu, *Macromol. Rapid Commun.* **2008**, *29*, 431–436; c) H. Li, W. Qi, H. Sun, P. Li, Y. Yang, L. Wu, *Dyes Pigm.* **2008**, *79*, 105–110.

[18] D. G. Kurth, P. Lehmann, D. Volkmer, A. Müller, D. Schwahn, *J. Chem. Soc. Dalton Trans.* **2000**, 3989–3998.

[19] J. Niu, X. You, C. Duan, H. Fun, Z. Zhou, *Inorg. Chem.* **1996**, *35*, 4211–4217.

[20] P. B. Rheiner, D. Seebach, *Chem. Eur. J.* **1999**, *5*, 3221–3236.

[21] a) R. A. MacPhail, H. L. Strauss, R. G. Snyder, C. A. Elliger, *J. Phys. Chem.* **1984**, *88*, 334–341; b) Q. Wang, B. Zhao, X. Zhang, J. Shen, Y. Ozaki, *Langmuir* **2002**, *18*, 9845–9852.

[22] J. W. Goodby, I. M. Saez, S. J. Cowling, V. Görtz, M. Draper, A. W. Hall, S. Sia, G. Cosquer, S. E. Lee, E. P. Raynes, *Angew. Chem.* **2008**, *120*, 2794–2828; *Angew. Chem. Int. Ed.* **2008**, *47*, 2754–2787.

[23] a) C. Tschierske, *J. Mater. Chem.* **1998**, *8*, 1485–1508; b) W. Li, J. Zhang, B. Li, M. Zhang, L. Wu, *Chem. Commun.* **2009**, 5269–5271.

[24] Z. Bo, X. Zhang, X. Yi, M. Yang, J. Shen, Y. Rehn, S. Xi, *Polym. Bull.* **1997**, *38*, 257–264.

Received: January 25, 2010
Published online: June 16, 2010

